

4*f* instability and elastic properties in the metal system TmS in high magnetic fields

Yoshiki Nakanishi,* Sakon Takuo, and Mitsuhiro Motokawa
Institute for Materials Research, Tohoku University, Sendai 980-8577, Japan

Takeshi Matsumura
Graduate School of Science, Tohoku University, Sendai 980-8578, Japan

Yuichi Nemoto, Hirofumi Hazama, and Terutaka Goto
Graduate School of Science and Technology, Niigata University, Niigata 950-2181, Japan

Takashi Suzuki
Institute for Solid State Physics, University of Tokyo, Tokyo 106-8666, Japan

(Received 22 December 2000; revised manuscript received 14 June 2001; published 23 October 2001)

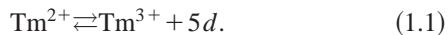
We have made an investigation of the elastic properties of TmS in high magnetic fields. A pronounced softening was observed in elastic constants C_{11} and $(C_{11} - C_{12})/2$ at low temperatures, while no softening was observed in C_{44} . An analysis based on crystalline electric field splitting of Tm ions indicates that ferroelectric quadrupolar interactions among quadrupolar moments with Γ_3 symmetry developed at low temperatures. Two distinct anomalies in C_{11} were found in magnetic fields. We propose an (H - T) phase diagram based on present and former results. This phase diagram implies that a field-induced ferromagnetic quadrupolar transition may occur in addition to an antiferromagnetic transition. Furthermore, the bulk modulus C_B exhibits a softening at low temperature, implying an instability of the 4*f* state in the Tm ions.

DOI: 10.1103/PhysRevB.64.184434

PACS number(s): 75.30.Kz, 75.30.Mb, 71.28.+d, 71.70.Ch

I. INTRODUCTION

Tm monochalcogenides (TmX: X=S, Se, Te), which crystallize in the simple NaCl structure, have attracted much attention because of their rich variety of magnetic and transport properties depending on X. These various phenomena such as metal-insulator transition, Kondo-like behavior in resistivity, metamagnetic transition in magnetization, and so on are mainly ascribed to the different degrees of instability of the 4*f* state in Tm ions.^{1,2} This instability causes a change of the valence of Tm ions is written as follows:²



The valence of Tm ion is related closely to the radius of the X ion as well as a lattice constant of TmX after crystallization. TmTe is a magnetic semiconductor with predominantly divalent Tm ions.³⁻⁶ The 4*f*¹³ level is located in the energy gap between 5*p* valence band and 5*d* conduction band.⁷⁻⁹ The higher valence band is mainly composed of chalcogenide and the *d* conduction band mainly of Tm. The difference in energy between the 5*d* conduction band and the 4*f*¹³ level is estimated to be 0.35 eV.¹⁰ As the lattice constant of TmX decreases, the crystalline electric field (CEF) effect on 5*d* conduction band becomes larger and making the 5*d* conduction band broader. At the same time the 4*f*¹³ level shifts to the higher energy side until the 4*f*¹³ level touches the bottom of 5*d* conduction band, at which point they hybridize. This situation is realized in TmSe. Tm ions are considered to fluctuate between two magnetic configurations Tm²⁺ and Tm³⁺ in TmSe.¹ Actually, it shows a homogenous intermediate-valence (IV) state.¹¹ Furthermore, in TmS, which has the smallest lattice constant in TmX, the 5*d* conduction band is

broader and the 4*f*¹³ level shifts more toward the higher energy side than those in TmSe. One electron which occupied the 4*f*¹³ level moves into the 5*d* conduction band. This sequential change in valency from Tm²⁺ to Tm³⁺ can be seen in the lattice parameter and Curie constant of these compounds.^{2,6,12} All of TmX shows the magnetic ordering at low temperatures. TmTe has an antiferromagnetic type II structure below $T_N = 0.4$ K,¹³ moreover, an antiferroelectric quadrupolar ordering seems to occur at $T_Q = 1.8$ K observed by specific heat measurement.⁴ TmSe has an antiferromagnetic type I structure below $T_N = 3.5$ K,¹¹ whereas below 6.5 K, TmS has an incommensurate modulated structure with a commensurate propagation $(\frac{1}{2}, \frac{1}{2}, \frac{1}{2})$ and an $(-\eta, \eta, 0)$ incommensurate vector, where $\eta = 0.075$ at 1.5 K.¹⁴

TmS has been studied intensively so far because it shows the following attractive phenomena. The resistivity exhibits anomalous behavior.³ That is to say, it follows mostly Kondo-like $\ln T$ dependence in the high temperature region, shows a maximum around 10 K, and a small jump at T_N . It peaks around 250 ($\mu\Omega$ cm) and remains constant at lower temperatures. However, this constant resistivity decreases in magnetic fields. The specific heat of TmS shows a sharp peak at T_N .³ This peak shifts to the lower temperature side with increase of magnetic fields. The corresponding entropy releases mostly $R \ln 2$ at T_N and then increases monotonously with increasing temperature. The plateau has not been seen because of the CEF splitting of 4*f* state in Tm ions. Some models of the CEF energy scheme have been proposed^{1,14-15} but the clear CEF splitting energy scheme has not been determined so far. The high temperature part of the thermal expansion of TmS indicates that CEF effects similar to those observed in TmSb might be present.¹ They imply a CEF splitting of the lowest two levels to be $\Gamma_1 - \Gamma_4$ of 25 K.

However, it seems that the total CEF splitting energy is small enough not to exhibit an anomaly in susceptibility measurements.^{3,6} Furthermore, the instability of Tm $4f$ state is considered to make it difficult to determine the explicit total CEF energy scheme.

In order to understand the nature of the $4f$ state in rare earth compounds, it is very important to determine the CEF level scheme of the $4f$ state in rare earth ions. Furthermore, again, a recent study on TmTe reveals that the quadrupolar moment plays an important role. Ultrasonic measurements are a powerful method to elucidate the ground state multiplet of rare earth ions split mainly by CEF effect, and the character of quadrupolar moments in $4f$ level.

Thus, a knowledge of the elastic properties measured by ultrasound is essentially important for understanding the $4f$ -electronic state in TmS and helps to explain the unusual features observed in TmS as mentioned above. In this paper, we report ultrasonic measurements under magnetic fields in the unusual metal TmS on a high quality single crystal sample. Brief reports have been published in Ref. 16.

II. EXPERIMENTS

The single crystal of TmS used in this study was grown by the Bridgman method in a tungsten crucible. Detailed information about the specimens are explained elsewhere.^{3,4} Each specimen used for the present ultrasonic measurement was cut into a rectangular along the $\langle 100 \rangle$ direction. For the measurement of the $(C_{11} - C_{12})/2$ mode, the plane (110) of a sample was polished using fine carborundum powder.

The sound velocity measurement was performed with an ultrasonic apparatus based on the phase comparison method. Piezoelectric transducers of quartz and LiNbO₃ were used. The fundamental resonance frequency of the quartz and LiNbO₃ is 10–30 MHz. The absolute velocity was obtained by measuring the delay time for a sequence of ultrasonic echoes with an accuracy of a several percent. The elastic constant $C = \rho v^2$ could be calculated from the sound velocity v and the density ρ of the crystal, ρ was estimated by the lattice constants of TmS ($a = 5.42 \text{ \AA}$).³ The measurement was carried out down to the temperature of 1.5 K and under magnetic fields up to 13 T using a superconducting magnet.

III. EXPERIMENTAL RESULTS

A. Temperature dependence of the elastic constants at zero field

We have measured the longitudinal as well as transverse ultrasonic modes. Figures 1 and 2 show the temperature dependence of the elastic constants C_{11} , $(C_{11} - C_{12})/2$, C_{44} , and C_B in TmS. The transverse C_{44} mode increases monotonously with decreasing temperature and shows a small dip around the antiferromagnetic ordering at $T_N = 6.5 \text{ K}$. However, the C_{44} shows an upward curvature. On the other hand, the longitudinal C_{11} mode exhibits a softening of 4.5% from 50 K down to the magnetic ordering point at T_N . The transverse $(C_{11} - C_{12})/2$ mode also exhibits a softening of 4.5% from 100 K down to T_N . This indicates that the CEF ground

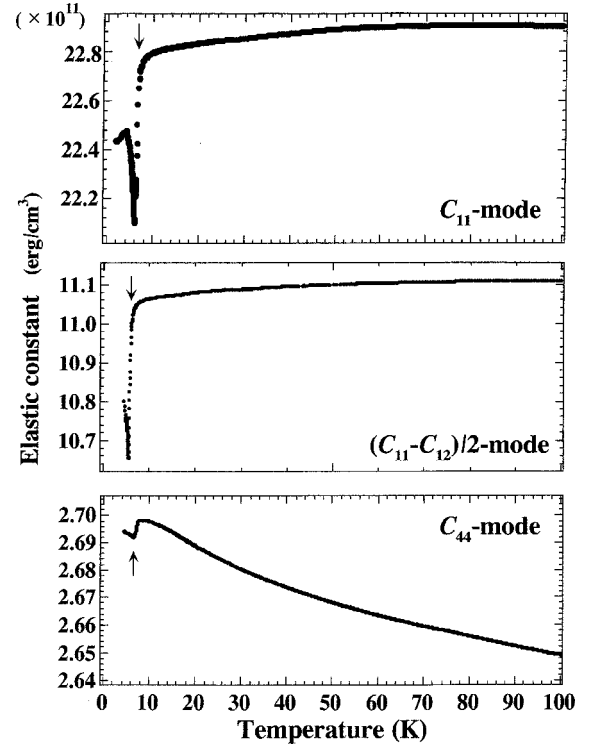


FIG. 1. Temperature dependence of the elastic constants C_{11} , $(C_{11} - C_{12})/2$, and C_{44} in TmS in zero field.

state has a degenerate quadrupolar moment with Γ_3 symmetry. To obtain information about the kind of quadrupolar interactions, the softening observed in $(C_{11} - C_{12})/2$ is analyzed using second order perturbation theory as discussed below. Moreover, the bulk modulus C_B associated with a volume strain $\epsilon^\alpha = (\epsilon_{xx} + \epsilon_{yy} + \epsilon_{zz})/\sqrt{3}$ calculated from C_{11} and $(C_{11} - C_{12})/2$ using the relation $C_B = (C_{11} + 2C_{12})/3$ exhibits a pronounced softening around T_N as shown in Fig. 2.

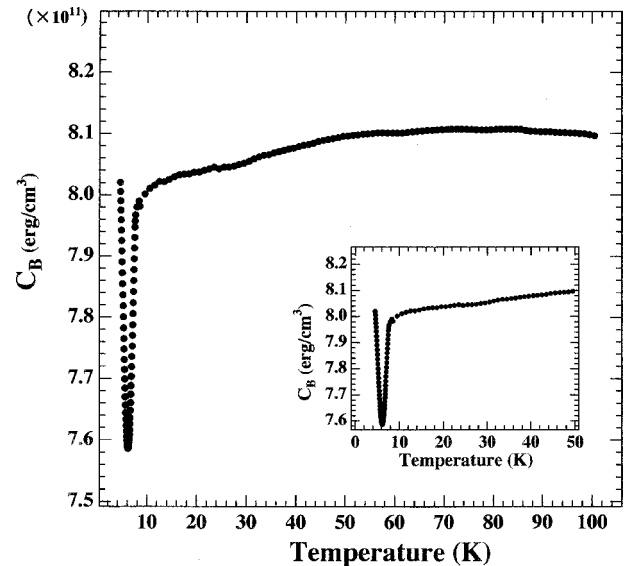


FIG. 2. Temperature dependence of bulk modulus C_B in TmS. The inset shows the temperature dependence of C_B on an expanded scale.

TABLE I. Expression of the quadrupolar operators, the normalized, symmetrized strains and the corresponding elastic constants for the cubic symmetry.

	$\varepsilon_{\Gamma\gamma}$	$O_{\Gamma\gamma}$	C_{Γ}
Γ_1	$\varepsilon^\alpha = (\varepsilon_{xx} + \varepsilon_{yy} + \varepsilon_{zz})/\sqrt{3}$	$O_B = J_x^2 + J_y^2 + J_z^2$	$C_{11} + 2C_{12} = 3C_B$
Γ_3	$\varepsilon_1^\gamma = (2\varepsilon_{zz} - \varepsilon_{xx} - \varepsilon_{yy})/\sqrt{6} = \varepsilon_u$ $\varepsilon_2^\gamma = (\varepsilon_{xx} - \varepsilon_{yy})/\sqrt{2} = \varepsilon_v$	$O_2^0 = \{3J_z^2 - J(J+1)\}/\sqrt{3}$ $O_2^2 = J_x^2 - J_y^2$	$(C_{11} - C_{12})$
Γ_5	$\varepsilon_1^e = \sqrt{2}\varepsilon_{yz}$ $\varepsilon_2^e = \sqrt{2}\varepsilon_{zx}$ $\varepsilon_3^e = \sqrt{2}\varepsilon_{xy}$	$O_{yz} = J_y J_z + J_z J_y$ $O_{zx} = J_z J_x + J_x J_z$ $O_{xy} = J_x J_y + J_y J_x$	$2C_{44}$

This result may suggest that volume instability occurs around T_N in this system. We will discuss about the volume effect in detail later.

Here, we consider the quadrupolar interaction between Γ_3 type quadrupolar moment associated with the softening observed in the transverse $(C_{11} - C_{12})/2$ mode. The interaction between the quadrupolar moment of the 4*f* electron and the elastic strain leads to elastic softening reflecting the CEF level scheme.

The Hamiltonian between the interaction of the quadrupolar moment $O_{\Gamma\gamma}$ in 4*f*-electronic state and the local strain $\varepsilon_{\Gamma\gamma}$ is shown as follows:^{17–20}

$$H_{qs} = \sum_i g_{\Gamma} O_{\Gamma\gamma}(i) \varepsilon_{\Gamma}, \quad (3.1)$$

where $O_{\Gamma\gamma}(i)$ is the equivalent quadrupolar operator at the *i*th rare earth site and g_{Γ} is the coupling constant. The suffix of Γ stands for the irreducible representation. The relation of the elastic strains, quadrupolar operators and corresponding elastic constants in cubic symmetry are summarized in Table I. From the second derivative of the free energy with respect to $\varepsilon_{\Gamma\gamma}$, the temperature dependence of the elastic constants is given by the following equation:

$$C_{\Gamma}(T) = C_{\Gamma}^0(T) - \frac{Ng_{\Gamma}^2\chi_{\Gamma}(T)}{1 - g_{\Gamma}'\chi_{\Gamma}(T)}, \quad (3.2)$$

where g_{Γ}' is the coupling constant between the quadrupolar moments and N is the number of ions in a unit volume. C_{Γ}^0 is the background elastic constant derived from non-*f*-electronic part. C_{Γ}^0 varies mainly because of anharmonic effects. The second term of Eq. (3.2) gives the effect of the localized *f* electrons in CEF level scheme. In the case of the ground state, which is degenerate with respect to the quadrupolar moment $O_{\Gamma\gamma}$, the corresponding elastic constant exhibits a softening in the nonzero Curie term. As mentioned in the Introduction, the explicit CEF energy level scheme of TmS has not been established yet. Thus, it is impossible to analyze our results in terms of Eq. (3.2), explicitly.

According to our results it is expected that the ground state degenerates with respect to O_2^0 or O_2^2 . The Curie term should be dominant at low temperatures. Together, they produce a pronounced softening. In this sense, therefore by using $\chi_{\Gamma} = A_{\Gamma}/T$, Eq. (3.2) is rewritten as follows:

$$C_{\Gamma}(T) = C_{\Gamma}^0(T) - \frac{Ng_{\Gamma}^2 A_{\Gamma}}{T - g_{\Gamma}' A_{\Gamma}}, \quad (3.3)$$

where A_{Γ} is the Curie constant of the quadrupolar susceptibility.¹⁸ The solid line of $(C_{11} - C_{12})/2$ shown in Fig. 3 is a fit with parameters of $Ng_{\Gamma}^2 A_{\Gamma} = 0.05$, $g_{\Gamma}' A_{\Gamma} = 5.5$. This means that $(C_{11} - C_{12})/2$ is almost governed by the Curie term in the elastic constant due to the ground state degenerated with the quadrupolar moment O_2^0 or O_2^2 . If Γ_3 doublet is the CEF ground state, the fitting curve gives us the $g_{\Gamma} = 2.64$ K and $g_{\Gamma}' = 0.266$ K. Thermal expansion of TmS is positive along the fourfold axis at T_N . Therefore, the O_2^0 -type ferroquadrupolar (FQ) interaction is considered to be dominant at lower temperatures.

B. Temperature dependence of the elastic constants under magnetic fields

Next, we would like to show the longitudinal elastic constant under magnetic fields up to 12 T along the $\langle 100 \rangle$ direction. Figure 4 shows the temperature dependence of C_{11} under magnetic fields along the $\langle 100 \rangle$ axis, in which a pronounced softening is observed at zero field. The softening

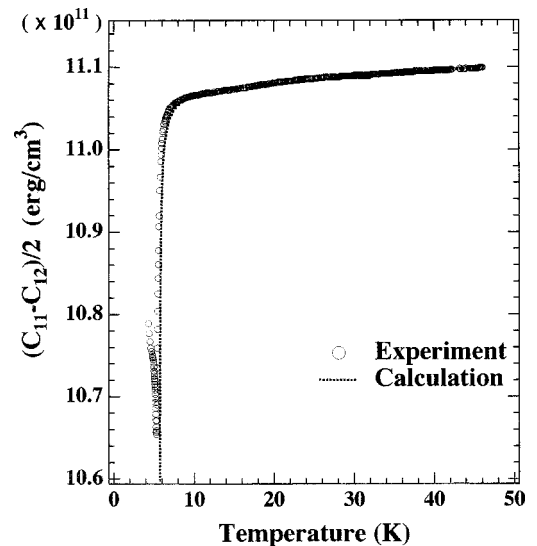


FIG. 3. Temperature dependence of the elastic constant $(C_{11} - C_{12})/2$ in TmS around T_N . Dotted line is a theoretical fit in terms of the formula (3.3) in the text. We obtain the parameters of $Ng_{\Gamma}^2 A_{\Gamma} = 0.05$, $g_{\Gamma}' A_{\Gamma} = 5.5$, and $C_{\Gamma}^0 = 11.07 \times 10^{11}$ (erg/cm³).

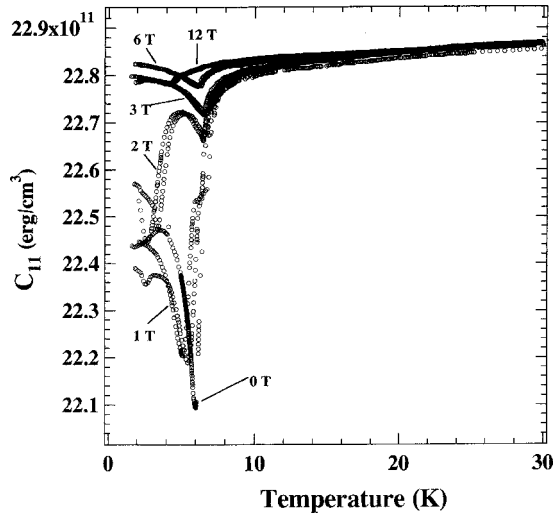


FIG. 4. Temperature dependence of C_{11} in TmS around T_N at various magnetic fields along the $\langle 001 \rangle$ axis.

observed around T_N is gradually suppressed with increasing magnetic fields. Figure 5 shows the detailed corresponding low temperature region in expanded scale. One anomaly around T_N is observed in zero field. However, by applying a magnetic field, this anomaly is split into two anomalies as shown in Fig. 5. The lower transition temperature shifts to lower temperatures with increasing fields and disappears around 2 T. While, the higher transition temperature shifts to higher temperatures up to 6 T and then shifts to lower temperatures above 6 T. The higher transition temperature becomes lower and gradually disappears with increasing magnetic fields. Both anomalies are considered to be related to the shift of the quadrupolar moment as will be discussed later.

Figure 6 shows the magnetic field dependence of C_{11} along the $\langle 100 \rangle$ direction at 1.5 and 4.2 K. The first-order

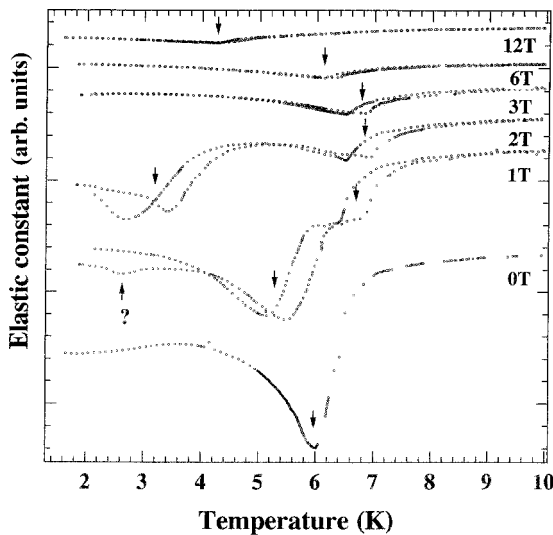


FIG. 5. Low-temperature behavior of the C_{11} mode of TmS in magnetic field on an expanded scale. Arrows indicate the transition temperatures.

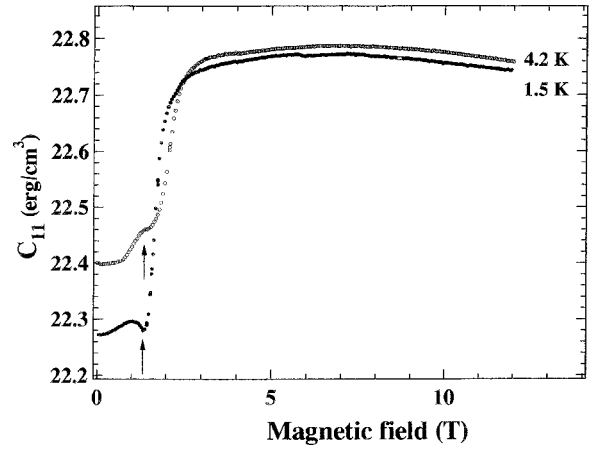


FIG. 6. Magnetic field dependence of C_{11} in TmS at 1.5 and 4.2 K. Arrow indicates the phase transition point.

phase transition occurs around 2 T accompanied with hysteresis. This result is consistent with a suppression of the softening under fields above 2 T as shown in Fig. 4.

C. (H - T) phase diagram

The (H - T) phase diagram of TmS was established from the present results and shown in Fig. 7. There are three different regions. An unusual feature of this phase diagram is that the boundary of phase I seems to disappear gradually with increasing magnetic fields. In our previous experiments, no anomaly could be detected by careful magnetization measurements in magnetic fields up to 30 T at this boundary as shown in Fig. 8.²¹ The boundary between phase II and phase III corresponds to the field where the softening is suppressed

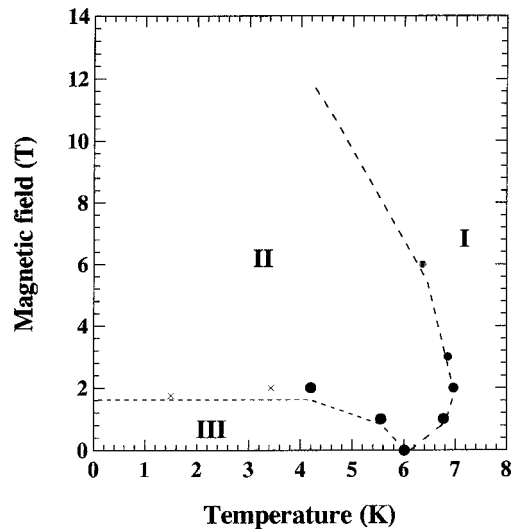


FIG. 7. Phase diagram of TmS in magnetic fields along the $\langle 001 \rangle$ axis. The darkness of closed circles represent the sharpness of anomalies in C_{11} - T measurement. The \times represents the anomaly in the C_{11} - H measurement. Phase I is a paramagnetic phase. Phase III is the antiferromagnetic phase. We propose that phase II might be a combined antiferromagnetic phase and field induced ferroquadrupolar ordering phase.

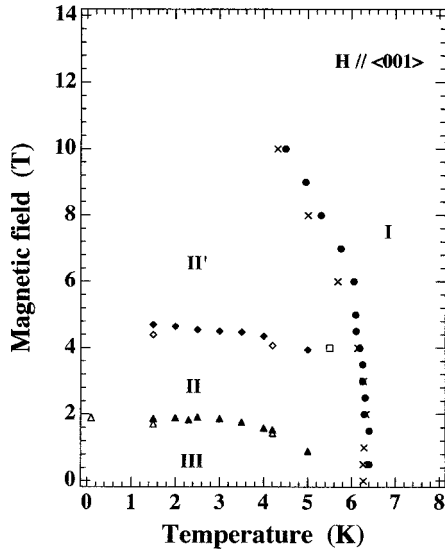


FIG. 8. The $(H-T)$ phase diagram for $H//\langle 001 \rangle$ determined by the former results. \times : specific heat (Ref. 21), \blacktriangle , \blacklozenge : magnetization (Ref. 25), \triangle , \diamond : magnetic resistance (Ref. 25), \bullet , \square : $M/H-T$ (Ref. 25).

rapidly by magnetic field. Also small anomaly has been observed in the magnetization at this point.

IV. DISCUSSION

From the analysis of the observed softening in C_{11} and $(C_{11} - C_{12})/2$, the CEF ground state of Tm ions in TmS has degenerate quadrupolar moments with Γ_3 symmetry and with a quadrupolar interaction among them. No softening has been observed in C_{44} , however, it exhibits upward curvature as a function of temperature. The same behavior has been observed in CeAs.²² Our present results also suggest that Γ_3 doublet is plausible as the CEF ground state of Tm ions in TmS. Actually, as mentioned in Introduction, the entropy releases mostly $R \ln 2$ at T_N indicating the CEF ground state to be doublet. Γ_3 ground state may bring a quadrupolar ordering. However, it is difficult to conclude at this moment that the CEF ground state is Γ_3 doublet because Γ_3 has no magnetic moment. If Γ_3 is the CEF ground state Γ_4 , $\Gamma_5^{(1)}$, or $\Gamma_5^{(2)}$ as an excited state will be needed to bring the magnetic ordering by the same story as a singlet-ground-state problem, where the interaction between thermally induced magnetic moments brings about the magnetic order. However, if $\Gamma_5^{(1)}$ or $\Gamma_5^{(2)}$ is chosen as the first excited state a softening must be observed in C_{44} . This is inconsistent with our present results. The explicit excited CEF energy scheme is still an open problem. Nevertheless, our results suggest that Γ_3 doublet is plausible as the CEF ground state.

As mentioned above, TmS has an AF magnetic structure with $q = [\frac{1}{2} + \eta, \frac{1}{2} - \eta, \frac{1}{2}]$, where η is 0.075 at 1.5 K.¹⁴ The magnetic moment is directed along one of the fourfolds axes.²³ This configuration is favorable for the ground state with Γ_3 symmetry. We expect that the FQ interaction of Γ_3 symmetry (O_2^0 -type) may cause the structural change. This

can exhibit a magnetic structure with a wave vector $q = [\frac{1}{2} + \eta, \frac{1}{2} - \eta, \frac{1}{2}]$ at low temperatures.

Next, we consider the $(H-T)$ phase diagram determined by the present results. There are three distinct phases. We expect that phase II may be O_2^0 -type FQ ordering induced by magnetic fields because of the following reasons. Present results indicate that the O_2^0 -type FQ interaction is dominant at low temperatures. The crystal stretches along the $\langle 100 \rangle$ axis at low temperatures.¹ The rapid hardening occurs at the transition between II and III. We made the $(H-T)$ phase diagram of TmS, using the results of magnetization, magnetoresistance, and specific heat measurements as shown in Fig. 8.^{21,24,25} It would be worthwhile to compare the two $(H-T)$ phase diagrams of TmS: Figs. 7 and 8. One can recognize the corresponding boundaries. The I phase boundary is determined by a well-defined elastic and specific heat anomaly. However, a small kink in magnetization is observed. There is another boundary in phase II, distinguished by II and II'. The phase boundary between II and II' is bounded by the abrupt decrease of magnetoresistance and the small anomaly in magnetization. However, this boundary has never been observed in the elastic constants. While the phase boundary between II and III is observed as an abrupt change in elastic constants and as a small anomaly in magnetization that it is recognized by dM/dH . In this system, we propose that both the magnetic and quadrupolar phases coexist. As described in a separate article of TmS, the exchange field was estimated.²¹ The degree of the exchange field corresponds well to the boundary between II and II' phase. Furthermore, we never observed the anomaly corresponding to this boundary via elastic constants. Thus, this boundary seems to be a magnetic boundary. On the other hand, at the phase boundary between II and III the softening of the elastic constant is suppressed by magnetic fields. This implies that a kind of phase transition occurs.

However, we cannot conclude that this phase is ferroquadrupole ordering, because some of the softening are not so large compared to conventional materials in which ferroquadrupole ordering occurs.^{18,26} Moreover, in TmS there is no remarkable lattice distortion observed in such materials.¹⁸ This may be related to the fact that the AF magnetic ordering occurs and the 4*f* state tends to be unstable around a transition temperature of 6.5 K, deduced from the temperature dependence of C_B presumably originating from the state with both configurations of Tm^{2+} and Tm^{3+} . These facts may affect the magnitude of the softening in C_{11} and $(C_{11} - C_{12})/2$ modes.

Here, we discuss magnetic ordering. The AF magnetic transition occurs at $T_N = 6.5$ K.¹⁴ However, it is not clear whether FQ ordering occurs or not in zero field. If both magnetic and quadrupolar ordering occur simultaneously at the same point, it should be a first order phase transition.²⁷⁻²⁹ This is not consistent with the results of specific heat measurements in magnetic fields. The obtained boundary between I phase and others seems to be second order.^{3,21} The obtained results let us conjecture that the magnetic phase transition causes the quadrupolar ordering.

Next, we must consider magnetic domain walls. The ro-

tation of a domain wall by magnetic fields also influences elastic constant. However, the softening cannot follow an analysis based on the Curie term of a quadrupolar strain susceptibility. In a thesis on TmS we suggest that the O_2^0 -type FQ interaction plays an important role in an anisotropy observed in magnetization curves, that is to say, the O_2^0 -type FQ interaction would be preferable to explain them.²¹ This consideration also leads the phase II and II' to be due to the O_2^0 -type FQ ordering induced by magnetic fields.

Finally, we comment the origin of a softening observed in C_B . The charge fluctuation of Tm ions seems to influence strongly C_B because it is related closely to a change of total volume as seen in the mixed valence system SmB₆.¹⁸ From the viewpoint of basic magnetism, it is very interesting how the valence changes below a magnetic transition temperature in intermediate-valence (IV) system. Especially, in TmS, both Tm²⁺ and Tm³⁺ have a magnetic moment originated from the 4*f* state different from Ce or Yb compounds. The IV state cannot be described by the usual *J* multiplet. The observed softening of C_B may be related to the change of a total volume of the crystal at low temperatures. The decision of a valence of Tm ions below 6.5 K will provide us crucial information to understand our result of C_B . The small magnitude of softening in C_{11} and $(C_{11}-C_{12})/2$ may be ascribed to the intermediate-valence 4*f* system. The electronic structure of TmS was determined by resonant photoemission studies.³⁰⁻³⁴ These results confirmed that the photoelectron spectra of TmS originates mostly from trivalent Tm 4*f* electrons with a small surface component of Tm²⁺ ions. However, no information about the bulk nature of TmS was reported. It is very difficult to remove the surface contributions in photoemission measurements. However, the magnetic susceptibility and recent neutron inelastic scattering measurements reveal that Tm ion has a valence of +2.9, not rigid +3.0.^{3,35} These results confirm that TmS has an intermediate-valence 4*f* state the same as TmSe.

V. CONCLUSION

We have performed ultrasonic investigation on TmS single crystal under magnetic fields. The elastic softenings

exhibit in C_{11} and $(C_{11}-C_{12})/2$, while monotonic increase of elastic constants has been appeared in C_{44} with decreasing temperature. The present results imply that the CEF multiplet ground state has degenerate quadrupolar moments with Γ_3 symmetry. We have found remarkable transitions in the elastic constant C_{11} under magnetic fields. The (*H-T*) phase diagram has been established by our results. We propose that the phases are composed of the AF magnetic phase and FQ-ordering phase. However, there remain unexplainable features associated with the boundary between I and others. We propose that AF interactions and O_2^0 -type FQ interactions coexists at low temperatures under magnetic field. In low fields the former is dominant, whereas above 2 T the latter is dominant and O_2^0 -type FQ ordering may occur, induced by magnetic fields.

Note that the bulk modulus C_B associated with the volume dependent strain exhibits anomalous softening as well as $(C_{11}-C_{12})/2$ presumably because of the valence instability of the 4*f* state. Around $T_N=6.5$ K magnetic ordering, the development of quadrupolar interactions between O_{Γ_3} and a valence instability occurred. The relatively small softening of C_{11} and $(C_{11}-C_{12})/2$ may be caused by valence fluctuations between Tm⁺² and Tm⁺³.

However, there still remains the fundamental question how the unstable 4*f* state produces the quadrupolar moment. We plan to measure the elastic constants of TmSe under magnetic fields. These results, especially to determine the (*H-T*) phase diagram, will help us to understand 4*f* properties in TmS and how the intermediate-valence state can bring about magnetic ordering as well as quadrupolar ordering of this material.

ACKNOWLEDGMENTS

One of the authors (Y.N.) would like to thank Professor H. Onodera and Dr. S. Nakamura for many stimulating discussions and for private communications. He would like to thank to Dr. Mumtaz Khalid for his help completing this manuscript.

*Present address: Department of Materials Science and Engineering, Iwate University, Morioka, 020-8551, Japan.

¹H. R. Ott, B. Lüthi, and P. S. Wang, *Valence Instabilities and Related Narrow Band Phenomena*, edited by R. D. Parks (Plenum, New York, 1977), p. 289.

²P. Wachter, *Handbook on the Physics and Chemistry of Rare Earths*, edited by K. A. Gschneidner, Jr., L. Eyring, G. H. Lander, and G. R. Choppin (Elsevier Science, British Vancouver, 1994), Vol. 19, p. 249.

³T. Matsumura, Ph.D. thesis, Tohoku University, 1996.

⁴T. Matsumura, S. Nakamura, T. Goto, H. Amitsuka, K. Matsuhira, T. Sakakibara, and T. Suzuki, *J. Phys. Soc. Jpn.* **67**, 612 (1998).

⁵T. Matsumura, H. Shida, and T. Suzuki, *Physica B* **230-232**, 738 (1997).

⁶E. Bucher, K. Andres, F. J. di Salvo, J. P. Maita, A. C. Gossard, A. S. Cooper, and G. W. Hull, Jr., *Phys. Rev. B* **11**, 500 (1975).

⁷N. Kioussis, B. R. Cooper, and J. M. Wills, *Phys. Rev. B* **44**, 10 003 (1991).

⁸E. Kaldis and P. Wachter, *Solid State Commun.* **11**, 907 (1972).

⁹B. Batlogg, E. Kaldis, A. Schlegel, and P. Wachter, *Phys. Rev. B* **14**, 5503 (1976).

¹⁰R. Suryanarayanan, G. Guntherodt, J. L. Freeouf, and F. Holtzberg, *Phys. Rev. B* **12**, 4215 (1975).

¹¹H. Bjerrum Møller, S. M. Shapiro, and R. J. Birgeneau, *Phys. Rev. Lett.* **39**, 1021 (1977).

¹²H. R. Ott and F. Hulliger, *Z. Phys. B: Condens. Matter* **49**, 323 (1983).

¹³Y. Lassailly, C. Vattier, F. Holtzberg, A. Benoit, and J. Flouquet, *Solid State Commun.* **52**, 717 (1984).

¹⁴Y. Lassailly, C. Vettier, F. Holtzberg, J. Flouquet, C. M. E. Zeyen, and F. Lapierre, *Phys. Rev. B* **28**, 2880 (1983).

¹⁵J. Peyrard, J. Flouquet, P. Haen, F. Lapierre, Y. Lassailly, F.

- Hotzberg, and C. Vettier, *J. Magn. Magn. Mater.* **31-34**, 433 (1983).
- ¹⁶Y. Nakanishi, F. Takahashi, T. Sakon, T. Matsumura, Y. Nemoto, H. Hazama, T. Goto, T. Suzuki, and M. Motokawa, *Physica B* **294-295**, 153 (2001).
- ¹⁷M. Kataoka and J. Kanamori, *J. Phys. Soc. Jpn.* **32**, 113 (1972).
- ¹⁸S. Nakamura, T. Goto, S. Kunii, K. Iwashita, and A. Tamaki, *J. Phys. Soc. Jpn.* **63**, 623 (1994).
- ¹⁹P. M. Levy, *J. Phys. C* **6**, 3545 (1973).
- ²⁰V. Dohm and P. Fulde, *Z. Phys. B* **21**, 369 (1975).
- ²¹Y. Nakanishi, T. Sakon, F. Takahashi, T. Matsumura, T. Suzuki, and M. Motokawa, *J. Phys. Soc. Jpn.* **70**, 2703 (2001).
- ²²K. Morita, Ph.D. thesis, Tohoku University, 1994.
- ²³Y. Lassailly, C. Vettier, F. Holtzberg, and P. Burlet, *Physica B* **136**, 391 (1986).
- ²⁴Y. Nakanishi, F. Takahashi, T. Sakon, H. Nojiri, M. Motokawa, T. Matsumura, and T. Suzuki, *Physica B* **259-261**, 329 (1999).
- ²⁵Y. Nakanishi, T. Sakon, F. Takahashi, T. Matsumura, T. Suzuki, and M. Motokawa, *Physica B* **281&282**, 595 (2000).
- ²⁶T. Goto, Y. Nemoto, Y. Nakano, S. Nakamura, T. Kajitani, and S. Kunii, *Physica B* **281&282**, 586 (2000).
- ²⁷J. Sivardiere and M. Blume, *Phys. Rev. B* **5**, 1126 (1972).
- ²⁸D. K. Ray and J. Sivardiere, *Solid State Commun.* **19**, 1053 (1976).
- ²⁹S. J. Allen, *Phys. Rev.* **167**, 492 (1968).
- ³⁰G. Kaindl, C. Laubschat, B. Reihl, R. A. Pollak, N. Mårtensson, F. Holtzberg, and D. E. Eastman, *Phys. Rev.* **167**, 492 (1968).
- ³¹G. Kaindl, C. Laubschat, B. Reihl, R. A. Pollak, N. Mårtensson, F. Holtzberg, and D. E. Eastman, *Valence Instabilities*, edited by P. Wachter and H. Boppert (North-Holland, Amsterdam, 1982), p. 281.
- ³²Y. Ufuktepe, S. Kimura, T. Kinoshita, K. G. Nath, H. Kumigashira, T. Takahashi, T. Matsumura, T. Suzuki, H. Ogasawara, and A. Kotani, *J. Phys. Soc. Jpn.* **67**, 2018 (1998).
- ³³K. G. Nath, Y. Ufuktepe, S. Kimura, T. Kinoshita, H. Kumigashira, T. Takahashi, T. Matsumura, T. Suzuki, H. Ogasawara, and A. Kotani, *J. Electron Spectrosc. Relat. Phenom.* **88-91**, 369 (1998).
- ³⁴T. Kinoshita, Y. Ufuktepe, K. G. Nath, S. Kimura, H. Kumigashira, T. Takahashi, T. Matsumura, T. Suzuki, H. Ogasawara, and A. Kotani, *J. Electron Spectrosc. Relat. Phenom.* **88-91**, 377 (1998).
- ³⁵T. Matsumura (private communication).